arXiv:2512.04629v1 [cs.AI] 4 Dec 2025

BioMedGPT-Mol: Multi-task Learning for Molecular Understanding and Generation

Chenyang Zuo[1] † **Siqi Fan**[1] † **Zaiqing Nie**[1,2] *
[1] Institute for AI Industry Research (AIR), Tsinghua University [2] PharMolix Inc.

Abstract

Molecules play a crucial role in biomedical research and discovery, particularly in the field of small molecule drug development. Given the rapid advancements in large language models, especially the recent emergence of reasoning models, it is natural to explore how a general-purpose language model can be efficiently adapted for molecular science applications. In this work, we introduce BioMedGPT-Mol, a molecular language model designed to support molecular understanding and generation tasks. By curating and unifying existing public instruction datasets, we have assembled a large-scale, comprehensive, and high-quality training dataset. The model is then fine-tuned through a meticulously designed multi-task learning framework. On a consolidated benchmark derived from LlaSMol, TOMG-Bench, and MuMOInstruct, BioMedGPT-Mol achieves remarkable performance. Our experimental results demonstrate that a general-purpose reasoning model can be effectively and efficiently post-trained into a professional molecular language model through a well-structured multi-task curriculum. Leveraging the power of it, we further explore retrosynthetic planning task, and the performance on RetroBench demonstrates its competitive capability of acting as an end-to-end retrosynthetic planner. We anticipate that our approach can be extended to other biomedical scientific domains.

1 Introduction

Molecules serve as the fundamental tokens of the language of chemistry, and accurate molecular understanding and effective molecule generation are essential for molecule-centric scientific discovery, particularly in the field of small molecule drug development. SMILES (Simplified Molecular Input Line Entry System) [48], a linear molecular notation that encapsulates the structure of chemical compounds, is widely used in both academic papers and patents. This widespread adoption enables large language models (LLMs) to naturally process molecular language. However, the distribution gap between molecular language and natural language necessitates the development of a specialized molecular language model to support molecule-centric research in a question-answering format [16, 57]. Moreover, this molecular language model, as an enhanced base LLM, can further facilitate biomedical multimodal tasks [29] and optical chemical structure understanding tasks [12].

With the rapid advancement of LLMs, general-purpose models have demonstrated their generalization capabilities and can be adapted to various research fields [26, 52]. The development of reasoning models has further shown great potential in scientific discovery [20, 15, 46]. Typically, a specialized expert model can be evolved from a general-purpose LLM through in-domain continuous pre-training, specific supervised fine-tuning (SFT), and well-designed reinforcement learning (RL). Although corpora for some research fields have been released [31], the available pre-training data remains finite

*Corresponding author. † Equal contribution. For any questions or discussions, please email {fansiqi, dair}@air.tsinghua.edu.cn.

Preprint. Under review.

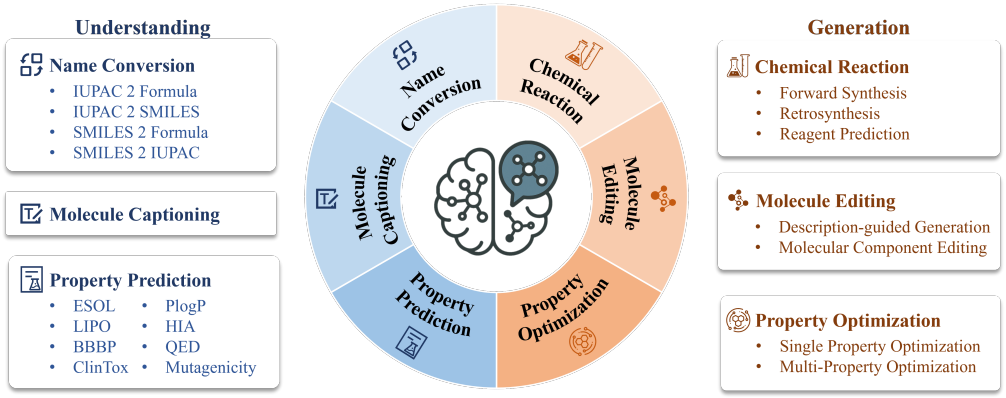

Figure 1: To facilitate molecule-centric scientific discovery, we introduce BioMedGPT-Mol, a molecular language model that simultaneously supports both molecular understanding and generation. Specifically, it is designed to address the following tasks: (1) Molecular understanding tasks, including name conversion, molecule captioning, and property prediction; (2) Molecular generation tasks, encompassing chemical reaction prediction, molecule editing, and property optimization. By integrating these capabilities, BioMedGPT-Mol aims to assist molecular research and development.

and limited. Consequently, the focus has shifted to reinforcement learning with verifiable rewards, particularly in the domain of mathematics [28, 5], and more recently in chemistry [33]. However, RL post-training remains computationally costly. Given the fast iterative evolution of open-source base LLMs, a natural question arises: Can we efficiently train a biomedical research assistant from a general-purpose reasoning LLM using only supervised fine-tuning? In this work, we explore this possibility in the field of molecular discovery.

Although SFT requires high-quality question-answering data pairs, the learning process is necessary to lead the model to imitate the behaviors of in-domain experts. Several publicly available instruction datasets already exist for molecule-centric scenarios [13, 54, 11, 25, 53, 9, 24]. However, existing works have primarily focused on specific aspects of molecular research, such as molecular understanding [13, 54], molecular editing [25], and property optimization [53, 25, 9]. The full potential of reasoning models in the entire molecular discovery journey has yet to be fully explored.

In this work, we first define the scope of a molecule-centric research assistant for biomedical scientific discovery, particularly for small molecule drug discovery. The molecular language model should address both molecular understanding and generation tasks, as illustrated in Figure 1. Thanks to several efforts in dataset construction, most of the required molecular tasks can be supported by existing public datasets, though they are scattered. We curate and unify these datasets to assemble a large-scale, comprehensive, and high-quality training dataset, comprising 13.6 million question-answering data pairs. To achieve general capability evolution across all relevant tasks, we design a multi-task learning strategy and utilize 5.8 million data pairs for supervised fine-tuning. This results in BioMedGPT-Mol, a molecular language model tailored for molecular discovery. Specifically, we introduce special tokens to help the model identify molecular language and enable controllable reasoning behaviors for molecular editing and optimization tasks. Finally, we consolidate a benchmark derived from LlaSMol [54], TOMG-Bench [25], and MuMOInstruct [9] to evaluate the model's general performance in molecular discovery scenarios. BioMedGPT-Mol achieves remarkable performance on this benchmark. The experimental results demonstrate that a general-purpose reasoning model can be effectively and efficiently post-trained into a specialized molecular language model through a well-structured multi-task curriculum.

Retrosynthetic planning is a fundamental problem in organic chemistry, aiming to identify a set of commercially available starting materials and a sequence of reactions that can synthesize a given target molecule. To the best of our knowledge, LLMs alone have not previously been deployed as effective multi-step retrosynthetic planners. In this work, we further explore this challenging task with BioMedGPT-Mol using a three-stage SFT strategy and demonstrate its competitive capability of acting as a fully end-to-end retrosynthetic planner on RetroBench [27].

We anticipate that our approach can be extended to other biomedical scientific domains to leverage the power of open-source reasoning models. Our contributions are summarized as follows:

- We define the scope of a molecule-centric research assistant for biomedical scientific discovery and introduce BioMedGPT-Mol, a molecular language model designed to advance molecular discovery.
- We present a multi-task learning strategy to enable the model to both understand and generate molecular language. The designed special tokens facilitate controllable reasoning behaviors for molecular editing and optimization tasks. Additionally, we assemble a large-scale, comprehensive, and high-quality dataset for training and consolidate a benchmark for evaluation.
- We validate the effectiveness of the proposed approaches through comprehensive experiments and demonstrate the performance advantages of BioMedGPT-Mol in the context of molecular discovery tasks.
- We are the first to explore the retrosynthetic planning task using an LLM alone, and we introduce a three-stage SFT strategy that enables BioMedGPT-Mol to function as an end-to-end retrosynthetic planner.

2 Related Work

Since the advent of large language models, they have been widely employed in chemistry applications[16, 49, 19]. Several recent efforts have focused on either fine-tuning LLMs with new datasets or conducting benchmark studies [54]. ChemLLM [57] introduces a framework featuring the first LLM dedicated to chemistry, including a dataset, ChemData, for training and a benchmark, ChemBench, for evaluation. Mol-Instructions [13] covers a broader range of biomolecular tasks and releases a larger instruction dataset. LlaSMol [54] is fine-tuned on SMolInstruct, a larger and more comprehensive dataset, achieving performance improvements. Molecule discovery involves not only understanding existing chemical compounds but also innovating and generating new ones. TOMG-Bench [25] evaluates LLMs on text-based open molecule generation and constructs an instruction tuning dataset, OpenMolIns. DrugAssistant [53] focuses on property optimization, while GeLLM3O [9] explores joint optimization for multiple properties. In contrast, ChemPile [31] presents a large-scale dataset for pretraining chemistry foundation models. Additionally, ether0 [33] is a chemistry reasoning model fine-tuned through reinforcement learning, and ChemCoTDataset [24] is released to enhance chemistry reasoning. The existing datasets are scattered, and the full potential of fine-tuned reasoning models in the entire molecular discovery journey has yet to be fully explored. We curate and unify these datasets to enhance general capabilities across all relevant molecular discovery tasks, resulting in BioMedGPT-Mol, a new molecular language model.

3 Problem Formulation

Accurate molecular understanding and effective molecule generation are crucial for molecule-centric scientific discovery. To develop a LLM-based research assistant that can facilitate molecular research, we first delineate the task scope, spanning from molecular understanding to generation.

3.1 Molecular Understanding Tasks

3.1.1 Name Conversion

Molecular name serves as the fundamental knowledge for molecular language. Name conversion [13, 54] requires the model to convert the name of a molecule from one representation to another, including converting IUPAC name to SMILES (I2S), converting IUPAC name to molecular formula (I2F), converting SMILES to IUPAC (S2I), and converting SMILES to molecular formula (S2F).

Example of Name Conversion Task - IUPAC 2 SMILES

Query: Can you give the SMILES notation of the molecule 4-N-(6-chloro-2-methoxyacridin-9-yl)-1-N,1-N-diethylpentane-1,4-diamine ?
Answer: Sure. CCN(CC)CCCC(C)NC1=C2C=CC(Cl)=CC2=NC2=CC=C(OC)C=C12

Example of Name Conversion Task - IUPAC 2 Formula

Query: Translate the chemical IUPAC name 4-N-(6-chloro-2-methoxyacridin-9-yl)-1-N,1-N-diethylpentane-1,4-diamine into its molecular formula.
Answer: C23H30ClN3O

Example of Name Conversion Task - SMILES 2 IUPAC

Query: Can you give the IUPAC name of the molecule CCN(CC)CCCC(C)NC1=C2C=CC(Cl)=CC2=NC2=CC=C(OC)C=C12?
Answer: Sure. 4-N-(6-chloro-2-methoxyacridin-9-yl)-1-N,1-N-diethylpentane-1,4-diamine.

Example of Name Conversion Task - SMILES 2 Formula

Query: I'd like to know the molecular formula of CCN(CC)CCCC(C)NC1=C2C=CC(Cl)=CC2=NC2=CC=C(OC)C=C12. Can you tell me?
Answer: Sure. It's C23H30ClN3O.

3.1.2 Molecule Captioning

Molecule captioning [13, 54, 11] involves generating a detailed textual description that elucidates the structure, properties, biological activity, and applications of a molecule based on its SMILES. By providing chemists and biologists with a quick and accessible summary of essential molecular information, it can efficiently guide their research and experimental efforts.

Example of Molecule Captioning Task

Query: I'd like a short overview about this molecule. Can you do that? CCCCCCCCCCCCCCCCCCCCCCCCCC(=O)O[C@H](COC(=O)CCCCCCCCCCCCCCCCCCCCCC)COP(=O)(O)OC[C@@H](O)COP(=O)(O)OC[C@@H](COC(=O)CCCCCCCCCC(C)CC)OC(=O)CCCCCCCCCCCC(C)C
Answer: The molecule is a stabilizing mitochondrial structure, proton trap for oxidative phosphorylation, cholesterol translocation that impacts barth syndrome and tangier disease. The molecule is a stabilizing cytochrome oxidase and a apoptosis that impacts aging, diabetic heart disease, and non-alcoholic fatty liver disease.

3.1.3 Property Prediction

Property prediction [50, 13, 54] involves estimating a molecule's inherent properties based on structural characteristics derived from its SMILES. By enabling the prediction of unknown attributes of new molecules, it may enhance research efficiency and reduces development times. It includes several subtasks.

plogP represents lipophilicity, balancing permeability, solubility, and metabolic stability. ESOL prediction [32] estimates water solubility, while Lipo prediction [35] assesses the octanol/water distribution coefficient, an important feature that influences both membrane permeability and solubility. Human Intestinal Absorption (HIA) prediction evaluates a molecule's ability to be absorbed through the gastrointestinal tract.

Example of Property Prediction - plogP

Query: Please predict the penalized octanol-water partition coefficient of [NH3+]C(CC1=c2cccc(O)c2=[NH+]C1)C(=O)[O-].
Answer: The penalized octanol-water partition coefficient is -7.84.

Example of Property Prediction - ESOL

Query: What is the logarithmic value of the solubility of CC#N in water?
Answer: 0.26 mol/L.

Example of Property Prediction - Lipo

Query: Provide the logD (the octanol/water distribution coefficient) at pH 7.4 of O=CC1=CC=CC=C1B(O)O.
Answer: 0.83.

Example of Property Prediction - HIA

Query: Please predict the intestinal adsorption of [NH3+]C(CC1=c2cccc(O)c2=[NH+]C1)C(=O)[O-].
Answer: The intestinal adsorption is 0.7.

The blood-brain barrier (BBB), which separates circulating blood from brain extracellular fluid, blocks most drugs, hormones, and neurotransmitters. This barrier presents a long-standing challenge in the development of drugs targeting the central nervous system (CNS). Blood-brain barrier penetration (BBBP) prediction involves two tasks: a classification task [30] to determine whether a molecule can cross the BBB, and a regression task to estimate the molecule's ability to cross. For CNS drug candidates, higher BBBP is desirable.

Example of Property Prediction - BBBP

Query: Is CNC(C)C(=O)C1=CC=C(OC)C=C1 capable of crossing the blood-brain barrier?
Answer: No.
Query: Please predict the BBB permeability of [NH3+]C(CC1=c2cccc(O)c2=[NH+]C1)C(=O)[O-].
Answer: The BBB permeability is 0.27.

QED (Quantitative Estimate of Drug-likeness) prediction is to predict the overall drug-likeness of a molecule by integrating multiple molecular attributes, including molecular weight, lipophilicity, and solubility.

Example of Property Prediction - QED

Query: Please predict the QED of [NH3+]C(CC1=c2cccc(O)c2=[NH+]C1)C(=O)[O-].
Answer: The QED is 0.48.

ClinTox prediction [14] is to predict whether the molecule is toxic to human body.

Example of Property Prediction - ClinTox

Query: Does CC(C)[NH2+]C(C)CC1=CC=C(I)C=C1 have toxicity?
Answer: No.

Mutagenicity (Mutag) prediction involves forecasting the likelihood that a drug will induce genetic mutations.

Example of Property Prediction - Mutag

Query: Predict the mutagenicity of [NH3+]C(CC1=c2cccc(O)c2=[NH+]C1)C(=O)[O-].
Answer: The mutagenicity is 0.2.

3.2 Molecular Generation Tasks

3.2.1 Chemical Reaction

The chemical reaction prediction task encompasses three subtasks: forward synthesis, retrosynthesis, and reagent prediction.

Forward reaction prediction [13, 54] aims to identify potential products given specific reactants and reagents. This subtask streamlines research and development processes reduces experimental guesswork.

Example of Chemical Reaction - Forward Synthesis

Query: C1CCOC1. CCN(CC)CC. CS(=O)(=O)Cl. CS(C)=O. N[C@@H]1CC2=CC=C(CN3C=C(CO)C(C(F)(F)F)=N3)C=C2C1 Considering the given starting materials, what might be the resulting product in a chemical reaction?
Answer: CS(=O)(=O)N[C@@H]1CC2=CC=C(CN3C=C(CO)C(C(F)(F)F)=N3)C=C2C1

Retrosynthetic analysis [13, 54] predicts potential reactants given a target product. This approach is crucial for designing efficient synthetic strategies for complex molecules, thereby accelerating the development of novel pharmaceuticals.

Example of Chemical Reaction - Retrosynthesis

Query: Based on the given product, provide some plausible reactants that might have been utilized to prepare it. N#CCC1=CC(Cl)=CC(CC2=NC3=C(F)C(F)=CC(F)=C3S2)=C1
Answer: N#CCC1=CC(Cl)=CC(CC#N)=C1.NC1=C(F)C(F)=CC(F)=C1S

Reagent prediction [13] focuses on identifying the appropriate catalysts, solvents, or auxiliary substances required for a specific chemical reaction. By doing so, it helps chemists optimize reaction conditions, ultimately enhancing the overall efficiency and cost-effectiveness of chemical processes.

Example of Chemical Reaction - Reagent Prediction

Query: Based on the given chemical reaction, can you propose some likely reagents that might have been utilized? O=CC1=CC([N+1](=O)[O-1])=C(F)C=C1F » O=[N+1]([O-1])C1=CC(CO)=C(F)C=C1F
Answer: C1CCOC1. Cl. [BH4-1]. [Na+1]

3.2.2 Molecule Editing

Molecule editing involves generating a new molecule that either meets a specific description or follows an explicit modification instruction. This task further comprises two main subtasks: description-guided generation and molecular component editing.

Description-guided molecule generation [13, 54] has the potential to streamline the process of molecular design by enabling the production of molecules that directly meet the criteria outlined in a given description. This approach facilitates a more targeted method for creating novel molecules, with applications in diverse fields such as drug discovery.

Example of Molecule Editing - Description-guided Generation

Query: Can you create a molecule that matches the given characteristics? The molecule is a branched amino pentasaccharide consisting of D-glucose at the reducing end having an alpha-L-fucosyl-(1->3)-[beta-D-galactosyl-(1->4)]-N-acetyl-beta-D-glucosaminyl-(1->3)-beta-D-galactosyl moiety attached at the 4-position. It is an amino pentasaccharide and a glucosamine oligosaccharide.
Answer: Sure. CC(=O)N[C@H]1[C@H](O[C@H]2[C@@H](O)[C@@H](CO)O[C@@H](O[C@H]3[C@H](O)[C@@H](O)C(O)O[C@@H]3CO)[C@@H]2O)O[C@H](CO)[C@@H](O[C@@H]2O[C@H](CO)[C@H](O)[C@H](O)[C@H]2O)[C@@H]1O[C@@H]1O[C@@H](C)[C@@H](O)[C@@H](O)[C@@H]1O.

Molecular component editing [25] is more straightforward and requires the model to make modifications to a given molecule, leveraging its knowledge of molecular structure. Specifically, the model is challenged to: (1) Add or remove a specific functional group, (2) Remove a designated functional group and then introduce a new one as specified to the molecule.

Example of Molecule Editing - Molecular Component Editing

Query: Add a hydroxyl to N#CC(=NNc1ccccc1)c1nc(-c2ccc3ccccc3c2)c(N=Nc2ccccc2)s1.
Answer: N#CC(=NNc1cccc(O)c1)c1nc(-c2ccc3ccccc3c2)c(N=Nc2ccccc2)s1
Query: Modify CC(C)Oc1cncc(NCc2c(C(F)(F)F)cnn2C)n1 by removing a halo.
Answer: CC(C)Oc1cncc(NCc2c(C(F)F)cnn2C)n1
Query: Please substitute a nitrile in COc1cccc2c(C)cc(SCC#N)nc12 with a halo.
Answer: COc1cccc2c(C)cc(SCI)nc12

3.2.3 Property Optimization

Property optimization tasks instruct the model to not only edit molecules but also to discern whether the modifications will steer the molecule toward a desired optimization target.

First, the model is tasked with optimizing a single property, such as logP, BBBP, MR (molecular refractivity), or QED, which pertains to the potential pharmacological attributes of the molecule.

Example of Property Optimization - Single Property Optimization

Query: Please modify the molecule NC(=[NH2+])c1ccc(N2CCC(c3ccccc3)C2)nc1 to increase its QED value.
Answer: NCc1ccc(N2CCC(c3ccccc3)C2)nc1.

Then, the model is challenged to jointly optimize multiple properties, which represent realistic challenges in lead optimization for drug development. Several representative properties are selected, including plogP, QED, BBBP, mutagenicity, and HIA.

Example of Property Optimization - Multi-Property Optimization

Query: Modify the molecule [NH3+]C(CC1=c2cccc(O)c2=[NH+]C1)C(=O)[O-] to increase its human intestinal adsorption ability value, decrease its mutagenicity value, increase its penalized octanol-water partition coefficient value, and increase its drug-likeness quantified by QED score value. Keep the modifications to the molecule structure as minimal as possible.
Answer: O=C([O-])C(CC1=c2cccc(O)c2=[NH+]C1)c1cccc(Br)c1

4 Methodology

Molecular understanding and generation can be regarded as the translation between molecular language and natural language. To enhance this process, we first introduce special tokens to help the model identify molecular language. We then employ multi-task learning to encourage the model to

capture the intrinsic distribution and enhance the generalization ability. Finally, we explore to enable controllable reasoning behaviors for molecular reasoning tasks, including editing and optimization.

4.1 Special Tokens for Molecular Language

We adopt several widely used special tokens to help the model identify the start and end of molecular language, following previous works [13, 54]. Specifically, there are three typical naming paradigms for a molecule: SMILES strings, IUPAC name, and molecular formula. These paradigms form the foundation of molecular language, and we introduce three corresponding tags to distinguish them.

- The <SMILES> </SMILES> tag is used to identify SMILES strings. It not only helps the model distinguish SMILES strings but also facilitates the parsing of generated molecules in molecular generation tasks.
- The <IUPAC> </IUPAC> tag is used to identify IUPAC names.
- The <MOLFORMULA> </MOLFORMULA> tag is used to identify molecular formula strings.

We preprocess the training data pairs to ensure that all SMILES strings, IUPAC names, and molecular formulas are enclosed within their corresponding tags.

4.2 Multi-task Learning Strategy

Although molecular understanding and generation tasks are diverse, they are interconnected and exhibit dependencies, as illustrated in Figure 2.

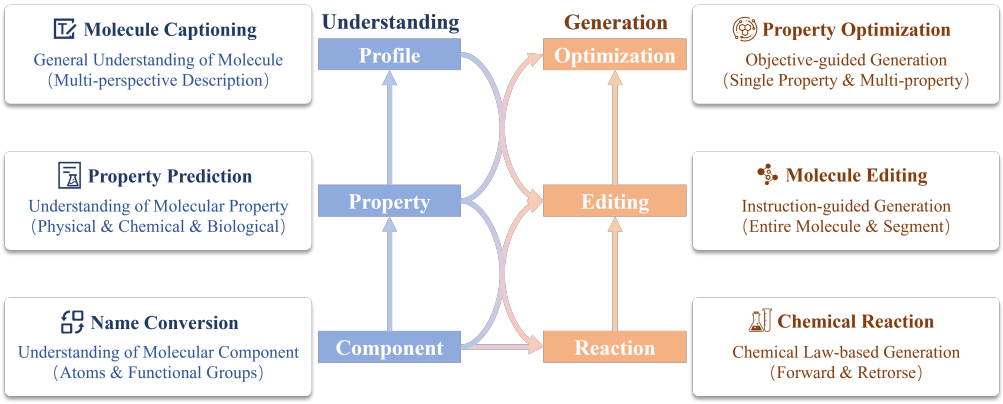

Figure 2: The various molecular tasks are interconnected, and multi-task learning enables molecular language models to capture the intrinsic essential attributes. Molecular understanding evolves from the concrete components of a molecule to its specific properties, and ultimately to an abstract, generalized description. Similarly, the guidance for molecule generation progresses from intrinsic chemical laws to detailed instructions, and then to specific property objectives. Accurate molecular understanding forms the foundation for effective molecule generation. In essence, better understanding leads to better generation.

SMILES strings, IUPAC names, and molecular formulas are the three typical naming paradigms in molecular language, each describing a molecule from a unique perspective. Molecular formulas represent a molecule at the atomic level, specifying the number of each type of atom present. SMILES strings provide additional structural information, organizing atoms according to the molecular structure, including functional groups. IUPAC names, which are readable by chemists, further introduce semantic information by incorporating the natural language names of functional groups. The name conversion task, as a foundational task, enables the model to understand molecular components from the atomic level to the structural level, and ultimately to the semantic level.

Building on the atomic components and structural characteristics derived from SMILES, the model is required to predict specific inherent properties, including physical, chemical, and biological properties.

This challenges the model to capture the relationship between structure and property. The model is then asked to provide a profile based on its understanding of molecular components and properties.

With an accurate understanding of existing molecules, the model is then challenged to learn to generate new ones. First, the chemical reaction prediction task requires the model to simulate chemical laws, leveraging its knowledge of molecular structure and properties. Next, the model is required to generate a molecule or modify segments of a given molecule based on detailed instructions. The model must understand both the composition of the molecule and the intention of the instructions. Finally, the model is encouraged to edit a given molecule to meet a specific property objective. This requires the model to predict the specific property of the source molecule, understand the optimization intention, and perform appropriate edits.

We employ a multi-task learning strategy to encourage the molecular language model to capture the intrinsic distribution and enhance its generalization ability for molecule-centric discovery.

4.3 A Large-scale, Comprehensive, and High-quality Dataset

To enable multi-task learning, we first review, curate, and unify existing molecule-related datasets, resulting in a large-scale, comprehensive, and high-quality dataset.

We adopt SMILES as the general molecular representation in all tasks except for name conversion, following the findings in [54]. During pre-processing, we enclose all SMILES strings, IUPAC names, and molecular formulas within their corresponding tags. To facilitate the property optimization task, we introduce auxiliary property prediction tasks, including plogP, QED, BBBP, Mutagenicity, and HIA regression tasks. The data pairs for these tasks are generated based on the raw property data provided in MuMOInstruct [9].

A detailed description of the reconstructed dataset is provided in Table 1.

Table 1: **Statistics of the Reconstructed Dataset.** cls: classification task. reg: regression task.

Category	Subcategory	Name	# K Pairs	Sources
Understanding	Name Conversion	I2S	299.9	SMolInstruct [54]
		I2F	299.9	SMolInstruct [54]
		S2I	299.9	SMolInstruct [54]
		S2F	299.9	SMolInstruct [54]
	Molecule Captioning	Molecule Captioning	205.7	SMolInstruct [54] L+M-24 [11]
	Property Prediction	ClinTox-cls	1.1	SMolInstruct [54]
		BBBP-cls	1.6	SMolInstruct [54]
		HIV-cls	32.9	SMolInstruct [54]
		Sider-cls	1.1	SMolInstruct [54]
		ESOL-reg	0.9	SMolInstruct [54]
		LIPO-reg	3.4	SMolInstruct [54]
		plogP-reg	1656.2	Constructed based on MuMOInstruct [9]
		QED-reg	1656.2	
		BBBP-reg	1656.2	
		Mutag-reg	1656.2	
		HIA-reg	1656.2	
Generation	Chemical Reaction	Forward Synthesis	971.8	SMolInstruct [54]
		Retrosynthesis	941.7	SMolInstruct [54]
		Reagent Prediction	125.4	Mol-Instructions [13]
	Molecule Editing	Description-guided Generation	56.5	SMolInstruct [54]
		Molecule Component Editing	55.7	OpenMolIns [25]
	Property Optimization	Single Property Optimization	885.9	MolOpt-Instruct [53]
		Multi-property Optimization	828.1	MuMOInstruct [9]
Total			$13,592.4$ **K** ≈ 13.6 **M**	

4.4 Controllable Behaviors for Molecular Reasoning

Although explicit reasoning (contents within the '<think>' tag) makes the model's behavior more explainable, it also introduces additional computational cost. In fact, not every task requires the inclusion of a 'thinking' process, even in molecular reasoning tasks. To enable users to manage and control reasoning behavior, we add 'thinking' data to molecular reasoning tasks, including molecular editing and property optimization. Inspired by Qwen3 [52], we adopt a 'no_think' flag to help the model recognize when to follow 'non-thinking' behavior.

Example of Molecular Editing in Thinking Behavior

Query: Add a carboxyl to the molecule CC1[NH2+]CCC1C(=O)Nc1cc(C(N)=O)ccc1Cl.
Answer: <think>

- Molecule Analysis: The input molecule contains a cyclohexane ring with an ammonium group ([NH2+]), a ketone (C=O), and an amide (C(=O)N) linked to a substituted benzene ring. The benzene ring has a urea-like group (C(N)=O) and a chlorine substituent. The primary functional groups are ammonium, ketone, amide, and urea.
- Editing Strategy: The benzene ring has available positions for substitution. The chlorine and urea-like groups are meta/para-directing. Adding a carboxyl group (-COOH) is most feasible at the meta position relative to the urea-like group (C(N)=O) to align with aromatic substitution patterns. This avoids steric hindrance and maintains electronic compatibility.
- Feasibility Analysis: While the benzene ring is deactivated by electron-withdrawing groups (Cl, C(N)=O), carboxylation via directed ortho/metalation or coupling reactions could achieve this modification. The proposed site (meta to C(N)=O) is chemically reasonable, though harsh conditions or specialized reagents may be required.

</think> CC1[NH2+]CCC1C(=O)Nc1cc(C(N)=O)cc(C(=O)O)c1Cl

Example of Single Property Optimization in Thinking Behavior

Query: Can you optimize the molecule C[N+]([O-])=Cc1cccc(Oc2ccccc2)c1 to improve its drug-likeness?
Answer: <think>

- Structural Analysis of the Molecule: The source molecule contains a nitro group ([N+]([O-])=C) attached to a methylene group, which is connected to a substituted benzene ring (diphenyl ether scaffold). The nitro group is electron-withdrawing and may contribute to high lipophilicity and metabolic instability.
- Property Analysis: The nitro group increases molecular weight, logP, and potential toxicity, reducing QED (drug-likeness). It also introduces a strong electron-withdrawing effect, which may hinder solubility and metabolic stability.
- Limitation in the Molecule for Property: The nitro group is a key limitation due to its negative impact on QED parameters (e.g., high logP, metabolic liability, and potential genotoxicity).
- Optimization for the Molecule: Replace the nitro group (-NO2) with a sulfonate ester (-SO3R), a bioisostere that reduces lipophilicity (lower logP), improves solubility, and eliminates nitro-related toxicity. The diphenyl ether scaffold is retained for structural integrity.

</think> CCS(=O)(=O)Oc1cccc(Oc2ccccc2)c1

To achieve this, we generate CoT (Chain of Thought) data pairs based on the raw data from ChemCoTDataset [24], which imitates experts' reasoning behaviors. For 'non-thinking' behavior, an empty thinking block is retained in the assistant's response to ensure internal format consistency. Similar to Qwen3, the model operates in thinking behavior by default. Examples of molecular reasoning tasks

in 'thinking' behavior are presented above. The statistics of the molecular CoT dataset are provided in Table 2.

Table 2: **Statistics of Molecular CoT Dataset.** cls: classification task. reg: regression task.

Category	Name	# K Pairs
CoT	Molecular Editing	4.5
	Single Property Optimization	2.8
Total		7.3

4.5 Implementation of BioMedGPT-Mol

We first construct the dataset for model fine-tuning, utilizing most of the data reported in Table 1. For the auxiliary property prediction tasks, we randomly sample $100,000$ data pairs for each task. The instructions of all these data pairs are concatenated with the '`no_think`' flag. Additionally, the generated CoT data pairs are integrated. In total, the entire training set comprises approximately 5.8 million question-answering pairs.

We initialize BioMedGPT-Mol with the pre-trained parameters of Qwen3-8B [52]. The model is fine-tuned for 3 epochs with a learning rate of 1×10^{-4} and a equivalent batch size of 256. To reduce training costs, we apply low-rank adaptation (LoRA) to BioMedGPT-Mol. Additionally, we perform linear warmup for the first 10% of steps and use a cosine annealing strategy to stabilize training. The entire training process requires approximately 624 GPU hours on Nvidia A800 GPUs.

5 Description of Benchmark

To evaluate the molecular language model's general performance in molecular discovery scenarios, we consolidate a benchmark derived from LlaSMol [54], TOMG-Bench [25], and MuMOInstruct [9].

5.1 Tasks

We select $58,904$ question-answering pairs across 19 representative tasks for practical applications such as small molecule drug discovery, covering a spectrum from molecular understanding to generation. The statistical information is reported in Table 3.

For molecular understanding, we include all four name conversion tasks (I2S, I2F, S2I, and S2F), the molecule captioning task, and four property prediction tasks (BBBP-cls, ClinTox-cls, ESOL-reg, and LIPO-reg). For molecular generation, we cover two chemical reaction tasks (forward synthesis and retrosynthesis), four molecule editing tasks (add component, delete component, substitute component, and description-guided generation), and four property optimization tasks.

Specifically, we select five multi-property optimization tasks from MuMOInstruct [9], which are independent of a specific target:

- BPQ (BBBP & plogP & QED) Joint Optimization: This task prioritizes brain permeability and appropriate lipophilicity while ensuring the optimized molecules retain favorable drug-like properties.
- MPQ (Mutagenicity & plogP & QED) Joint Optimization: This scenario represents early-stage lead optimization, aiming to reduce genotoxic risks while ensuring adequate lipophilicity and drug-like properties.
- BHMQ (BBBP & HIA & Mutagenicity & QED) Joint Optimization: Particularly relevant for orally administered central nervous system (CNS) drugs, this task emphasizes both brain and intestinal absorption as critical factors.
- BMPQ (BBBP & Mutagenicity & plogP & QED) Joint Optimization: This task reflects CNS drug design by balancing adequate lipophilicity, reduced toxicity, and favorable drug-like properties, simulating realistic requirements for CNS-active drugs.
- HMPQ (HIA & Mutagenicity & plogP & QED) Joint Optimization: This task represents optimization for orally administered drugs, focusing on absorption, genotoxic risk reduction, and overall drug-like quality.

Table 3: **Statistics of the Consolidated Benchmark.** cls: classification task. reg: regression task.

Category	Subcategory	Name	# Pairs	Sources
Understanding	Name Conversion	I2S	2,993	SMolInstruct [54]
		I2F	2,993	SMolInstruct [54]
		S2I	2,993	SMolInstruct [54]
		S2F	2,993	SMolInstruct [54]
	Molecule Captioning	Molecule Captioning	2,538	SMolInstruct [54]
	Property Prediction	ClinTox-cls	144	SMolInstruct [54]
		BBBP-cls	197	SMolInstruct [54]
		ESOL-reg	112	SMolInstruct [54]
		LIPO-reg	420	SMolInstruct [54]
Generation	Chemical Reaction	Forward Synthesis	4,062	SMolInstruct [54]
		Retrosynthesis	4,156	SMolInstruct [54]
	Molecule Editing	Add Component	5,000	TOMG-Bench [25]
		Delete Component	5,000	TOMG-Bench [25]
		Substitute Component	5,000	TOMG-Bench [25]
		Description-guided Generation	2,493	SMolInstruct [54]
	Property Optimization	logP Optimization	5,000	TOMG-Bench [25]
		QED Optimization	5,000	TOMG-Bench [25]
		MR Optimization	5,000	TOMG-Bench [25]
		Multi-property Optimization	2,810	MuMOInstruct [9]
Total			$58,904$	

5.2 Evaluation Metrics

We adopt the original evaluation metrics for each task , following [54, 25, 9].

Name Conversion Tasks. The exact match (EM) metric is adopted to measure whether the predictions exactly match the gold standards. We apply the following criteria: (1) SMILES strings are parsed into molecules, and they are considered a match only if the two molecules are identical; (2) Molecular formulas are determined to be a match if the set of atoms is the same and the corresponding numbers of each atom are identical; (3) For IUPAC names, the set composed of multiple parts separated by semicolons is compared to determine a match.

Molecule Captioning Task. As a natural language generation task, we employ text-based metrics to measure similarity, including METEOR, BLEU-2, BLEU-4, ROUGE-1, ROUGE-2, and ROUGE-L.

Property Prediction Tasks. We calculate the accuracy (Acc.) for binary classification tasks and use the root mean square error (RMSE) to measure the differences between predicted and actual values for regression tasks.

Chemical Reaction Tasks. To evaluate the generated molecules, we use three metrics: (1) Exact match (EM) indicates the proportion of predicted molecules that exactly match the gold standards; (2) Fingerprint Tanimoto Similarity (FTS) quantifies the structural similarities using the Tanimoto similarity of their Morgan fingerprints; (3) Validity (Valid) measures the ratio of valid molecules generated, following SMILES grammar and chemical valence rules.

Molecule Editing. We employ the EM, FTS, and Valid metrics to measure the performance in the description-guided generation task. For component editing tasks, we adopt the success rate (SR), which is the percentage of molecules that successfully pass the rigorous testing processes [25]. The testing process, developed with RDKit, compares the generated molecule with the original one and verify whether the number of specified functional groups is correct after the required modification.

Property Optimization. We also adopt the success rate (SR) as a metric to indicate the proportion of generated molecules for which the specified property or all desired properties are successfully optimized as required. For each multi-property optimization instruction, we generate 20 molecules via beam search decoding, following the evaluation setting in [9].

6 Experiments

We evaluate BioMedGPT-Mol on molecular understanding and generation tasks and compare its performance with other models. BioMedGPT-Mol shows remarkable performance in molecular discovery scenarios.

6.1 Molecular Understanding

Firstly, we evaluate the model's capabilities in component recognition, specific property prediction, and profile generation.

Across all LLMs, BioMedGPT-Mol achieves the best performance on name conversion (Table 4), molecule captioning (Table 5), and property prediction (Table 6). It not only surpasses general-purpose LLMs (GPT-4 [1], Claude-3 Opus [3], and Galactica [45]) by substantial margins, but also outperforms the three chemistry LLMs (MolInst [13], ChemLLM [57], and LlaSMol [54]), underscoring its mastery of molecular language.

On name conversion (Table 4), BioMedGPT-Mol improves over LlaSMol by an absolute 7% EM on average, evidencing its strong component-level understanding, which is the foundation of molecular understanding. For general LLMs, this task remains challenging; Claude-3 Opus attains only 15.4% average EM. For reference, we follow [54] and include task-specific baselines: STOUT [36], an encoder-decoder model specifically trained on SMILES–IUPAC pairs, handles I2S and S2I; a deterministic RDKit routine covers S2F; and I2F is decomposed into I2S+S2F. BioMedGPT-Mol has further narrowed the gap between LLMs and these specialized solutions.

Table 4: **Performance on Name Conversion.** RDKit and STOUT [36] are used as SOTA task-specific models [54]. All the EM scores are in %. The best performances of LLM-based models are highlighted in bold.

Methods	Avg.	I2F	I2S	S2F	S2I
Task Specific, Non-LLM based Models					
SOTA	82.0	97.9	73.5	100	56.5
General LLM					
GPT-4 [1]	4.2	8.7	3.3	4.8	0.0
Galactica [45]	4.7	9.1	9.7	0.0	0.0
Claude3 Opus [3]	15.4	34.6	17.7	9.2	0.0
Chemistry LLM					
Molinst [13]	0.0	0.0	0.0	0.0	0.0
ChemLLM [57]	0.3	0.8	0.3	0.0	0.0
LlaSMol [54]	70.1	87.9	70.1	93.2	29.0
BioMedGPT-Mol	**77.1**	**91.4**	**76.5**	**95.7**	**44.9**

Table 5: **Performance on Molecule Captioning.** BL: BLEU. R: ROUGE. The best performances of LLM-based models are highlighted in bold.

Methods	METEOR	BL-2	BL-4	R-1	R-2	R-L
Task Specific, Non-LLM based Models						
Mol-T5 [10]	0.515	0.462	0.366	0.563	0.398	0.501
General LLM						
Galactica [45]	0.050	0.018	0.002	0.061	0.012	0.052
GPT-4 [1]	0.188	0.095	0.020	0.238	0.058	0.156
Claude3 Opus [3]	0.219	0.114	0.030	0.263	0.069	0.173
Chemistry LLM						
ChemLLM [57]	0.050	0.012	0.004	0.057	0.005	0.048
Molinst [13]	0.124	0.028	0.020	0.226	0.160	0.217
LlaSMol [54]	0.452	0.414	0.319	0.521	0.357	0.463
BioMedGPT-Mol	**0.515**	**0.477**	**0.381**	**0.562**	**0.403**	**0.501**

Table 6: **Performance on Property Prediction.** The fine-tuned Uni-Mol [59] is used as SOTA task-specific models [54]. All the accuracy scores are in %. The best performances of LLM-based models are highlighted in bold.

Methods	Avg.-reg	ESOL	LIPO	Avg.-cls	BBBP	ClinTox
	RMSE ↓	RMSE ↓	RMSE ↓	Acc.	Acc.	Acc.
Task Specific, Non-LLM based Models						
Uni-Mol [59]	0.716	0.819	0.612	88.9	85.3	92.4
General LLM						
GPT-4 [1]	2.058	2.570	1.545	56.5	62.9	50.0
Claude3 Opus [3]	1.115	1.036	1.194	58.4	75.1	41.7
Galactica [45]	3.582	4.184	2.979	80.7	69.0	92.4
Chemistry LLM						
Molinst [13]	1.981	2.271	1.691	33.6	60.9	6.3
ChemLLM [57]	1.872	1.946	1.797	49.0	22.3	75.7
LlaSMol [54]	1.080	1.150	1.010	83.9	74.6	**93.1**
BioMedGPT-Mol	**0.945**	**0.916**	**0.973**	**90.4**	**87.6**	**93.1**

In molecule captioning (Table 5), BioMedGPT-Mol records a METEOR score of 0.515, outperforming LlaSMol [54] (0.452) and Claude-3 Opus [3] (0.219). Compared with the task-specific Mol-T5 [10] baseline, BioMedGPT-Mol delivers competitive performance.

Property prediction (Table 6) comprises both regression and classification tasks. For regression (ESOL and LIPO), BioMedGPT-Mol attains an average RMSE of 0.945, demonstrating strong modeling of intrinsic properties. On classification, it reaches 90.4% average accuracy, ranking first among all LLMs and even surpasses the task-specific baseline Uni-Mol [59]. These experimental results underscore the model's grasp of the intricate links among molecular components, structure, and properties.

6.2 Molecular Generation

Next, we assess the model's capabilities in three areas: intrinsic chemical law-based generation, detailed instruction-guided generation (description-guided generation and molecular component editing), and specific property objective-guided generation. Benefiting from its superior molecular understanding capabilities, BioMedGPT-Mol outperforms both general LLMs and chemistry-specific LLMs on these molecular generation tasks, as shown in Table 7, 8, 9, 10, and 11.

Table 7: **Performance on Chemical Reaction.** RSMILES [58] and Molecular Transformer [38] are re-trained as the SOTA task-specific models for forward synthesis and retrosynthesis respectively [54]. All the reported scores are in %. The best performances of LLM-based models are highlighted in bold.

Methods	Avg.	Forward Synthesis			Retrosynthesis		
	EM	EM	FTS	Valid	EM	FTS	Valid
Task Specific, Non-LLM based Models							
SOTA	62.9	78.7	92.2	100.0	47.0	77.5	99.7
General LLM							
Galactica [45]	0.0	0.0	25.9	83.7	0.0	34.6	93.0
GPT-4 [1]	0.8	1.6	40.5	87.0	0.0	33.4	42.6
Claude3 Opus [3]	2.4	3.7	45.7	97.0	1.1	46.2	94.8
Chemistry LLM							
ChemLLM [57]	0.0	0.0	1.6	38.5	0.0	2.9	10.9
Molinst [13]	3.9	2.1	31.7	**99.8**	5.7	48.0	97.8
LlaSMol [54]	48.1	63.3	84.9	**99.8**	**32.9**	70.4	**100.0**
BioMedGPT-Mol	**49.8**	**67.2**	**88.5**	**99.8**	32.4	**75.2**	99.9

We evaluate BioMedGPT-Mol on forward synthesis and retrosynthesis tasks (Table 7) to assess its understanding of intrinsic chemical laws, which underpins all molecular generation tasks. BioMedGPT-Mol achieves the best overall performance among all LLMs, with an average EM score of 49.8%.

General LLMs struggle to capture in-domain rules, resulting in unsatisfactory performance. Even the two chemistry LLMs, Molinst [13] and ChemLLM [57], face challenges with these tasks. LlaSMol [54] achieves an average EM score of 48.1% and performs better on retrosynthesis. For reference, two transformer-based encoder-decoder models, RSMILES [58] and Molecular Transformer [38], specifically adapted for these tasks, serve as task-specific baselines [54]. A performance gap persists between LLM-based approaches and specialized solutions. Further research is needed to enhance the capabilities of LLMs and narrow this gap.

Table 8: **Performance on Description-guided Generation.** All the reported scores are in %. The best performances of LLM-based models are highlighted in bold.

Methods	EM	FTS	Valid
Task Specific, Non-LLM based Models			
Mol-T5 [10]	31.7	73.2	95.3
General LLM			
Galactica [45]	0.0	11.6	94.7
GPT-4 [1]	6.4	42.6	81.4
Claude3 Opus [3]	12.3	57.6	92.6
Chemistry LLM			
ChemLLM [57]	0.9	14.3	4.3
Molinst [13]	6.0	43.6	84.8
LlaSMol [54]	19.2	61.7	**99.7**
BioMedGPT-Mol	**29.6**	**77.5**	98.9

For description-guided molecular generation (Table 8), models are tasked with generating a molecule that fits the given description. BioMedGPT-Mol achieves an EM score of 29.6% and a FTS score of 77.5%, surpassing LlaSMol [54] by 10.4% and 15.8%, respectively. Given the open-ended nature of this generation task, molecules that do not exactly match the gold standard may still be considered acceptable. BioMedGPT-Mol excels in FTS similarity score, even outperforming the task-specific baseline Mol-T5 [10]. Experimental results highlight its strong capability in translating between natural language and molecular language.

Table 9: **Performance on Molecular Component Editing.** All the SR scores are in %. The best performances of LLM-based models are highlighted in bold.

Methods	Avg.	Add Comp.	Delete Comp.	Sub. Comp.
Task Specific, Non-LLM based Models				
Bio-T5 [34]	19.4	34.6	16.7	6.8
Mol-T5 [10]	22.5	28.3	22.3	16.9
General LLM				
Claude3.5 [4]	67.8	68.3	54.1	**81.0**
GPT-4o [1]	70.6	61.9	70.1	79.9
Gemini-1.5-pro [8]	72.6	70.6	75.9	71.5
GPT-4-turbo [1]	73.4	69.9	72.4	77.8
Chemistry LLM				
OpenMolIns-125M [25]	47.5	58.4	65.3	18.7
OpenMolIns-8B [25]	54.5	58.2	51.0	54.4
BioMedGPT-Mol	**74.2**	**72.9**	**88.4**	61.3

Unlike generation from scratch, molecular component editing (Table 9) demands a understanding of molecular structural components and editing instructions to execute modifications effectively. General LLMs show promising performance in this area. GPT-4 Turbo [1] stands out as the top performer, achieving an average success rate of 73.4%. However, the performance of the existing chemistry LLM, OpenMolIns [25], highlights the considerable room for improvement. BioMedGPT-Mol achieves a remarkable success rate of 74.2%, surpassing GPT-4 Turbo. Despite these advancements, there is still room for improvement, especially in the substitution task, where Claude3.5 [4] demonstrates a significant advantage.

Property optimization tasks (Table 10) require models to steer molecules toward desired optimization targets, necessitating a deeper understanding of the relationship between molecular structure and

Table 10: **Performance on Single Property Optimization.** All the SR scores are in %. The best performances of LLM-based models are highlighted in bold.

Methods	Avg.	logP	MR	QED
Task Specific, Non-LLM based Models				
Mol-T5 [10]	44.6	42.4	45.0	46.5
Bio-T5 [34]	51.0	51.6	50.6	50.7
General LLM				
GPT-4o [1]	60.0	71.9	68.6	39.5
GPT-4-turbo [1]	63.3	76.6	73.9	39.5
Claude3.5 [4]	67.6	79.7	69.6	53.6
Gemini-1.5-pro [8]	67.6	77.1	78.8	47.0
Chemistry LLM				
OpenMolIns-125M [25]	67.6	73.6	71.2	57.9
OpenMolIns-8B [25]	68.0	80.5	71.2	52.2
BioMedGPT-Mol	**77.2**	**87.9**	**80.0**	**63.8**

properties. BioMedGPT-Mol excels in all three subtasks, achieving an average success rate of 77.2%, which outperforms the second-best model, OpenMolIns-8B [25], by 9.2%. The experimental results highlight BioMedGPT-Mol's ability to provide critical insights into the potential pharmacological attributes of molecules, thereby assisting chemists in identifying viable drug candidates.

Table 11: **Performance on Multi-property Optimization.** All the SR scores are in %. The best performances of LLM-based models are highlighted in bold.

Methods	Avg.	BPQ	MPQ	BHMQ	BMPQ	HMPQ
General LLM (0-shot)						
Mistral [2]	14.8	15.8	11.2	12.7	12.6	21.9
GPT-4o [1]	23.9	36.4	19.4	17.8	25.1	20.8
Claude3.5 [4]	49.8	56.0	17.4	39.0	44.5	38.5
General LLM (few-shot)						
GPT-4o [1]	25.0	40.0	21.4	14.4	24.1	25.0
Mistral [2]	51.8	68.6	59.6	34.8	49.2	46.9
Claude3.5 [4]	59.6	76.8	50.6	39.0	44.5	38.5
Chemistry LLM						
ChemLLM [57]	4.2	4.8	6.2	1.7	5.2	3.1
LlaSMol [54]	66.8	86.0	76.4	53.4	64.9	53.1
GeLLM3O-mistral [9]	92.2	96.8	**95.2**	86.4	91.1	91.7
GeLLM3O-llama [9]	95.0	95.0	93.6	**93.2**	**95.3**	**97.9**
BioMedGPT-Mol	**95.2**	**99.2**	94.6	**93.2**	94.2	94.8

Multi-property joint optimization further challenges models to improve all required properties simultaneously, necessitating the balancing of multiple trade-offs and conflicting objectives. BioMedGPT-Mol substantially outperforms general LLMs by a large margin, achieving a significant average improvement of 59.7% in success rate over the best general LLM baseline, Claude 3.5 (5-shot) [4]. Fine-tuned with specialized knowledge, the chemistry LLMs designed for property optimization, GeLLM3Os [9], exhibit remarkable performance with success rates of 92.2% and 95.0% for two different versions. BioMedGPT-Mol surpasses them in overall performance, achieving a success rate of 95.2%, which underscores its potential for applications in lead optimization.

6.3 Performance Advantage of Explicit Reasoning on Molecular Component Editing

We further investigate a representative molecule-centric reasoning task, molecular component editing, to examine the performance differences between explicit and implicit reasoning behaviors, in other words, 'thinking' and 'non-thinking'. BioMedGPT-Mol allows users to manage and control reasoning behavior. We evaluate the model's performance on the editing task with explicit reasoning enabled. The performance comparison between the two reasoning behaviors is shown in Figure 3. Explicit reasoning behavior effectively improves performance across all three subtasks, resulting in an average success rate of 79.0%. The performance improvement on the 'add component' task is particularly

significant, with explicit reasoning outperforming implicit reasoning by 11.6%, setting a new state-of-the-art level. This highlights the potential power of molecular language models on reasoning tasks through increased inference computation budget.

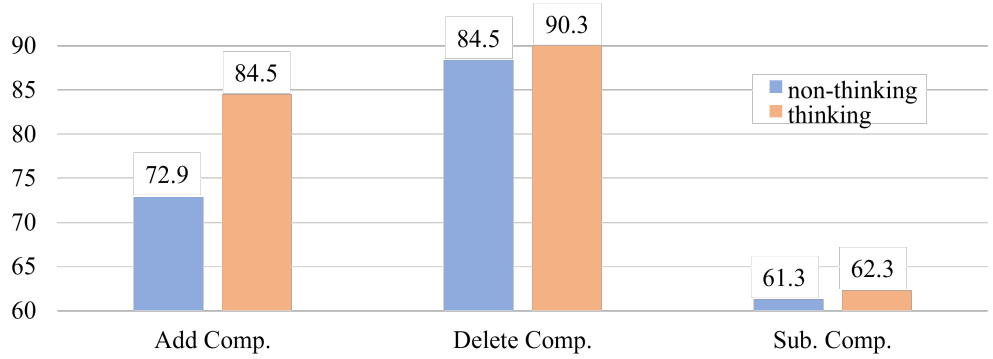

Figure 3: Performance comparison between non-thinking and thinking behavior on molecular component editing task.

7 Further Exploring Retrosynthetic Planning with BioMedGPT-Mol

Leveraging the power of BioMedGPT-Mol, we further explore retrosynthetic planning task.

Multi-step retrosynthetic planning is a fundamental problem in organic chemistry. It aims to identify a set of commercially available starting materials and a sequence of reactions to synthesize a given target molecule. Although recent works explore direct route generation to mitigate the exponential search space [41], existing deep learning-based methods predominantly employ iterative search algorithms [40, 6, 23, 56, 51, 17, 18, 55]. Starting from the target, they iteratively select and deconstruct molecules until a viable set of starting materials is obtained. By integrating a policy network, Monte Carlo Tree Search (MCTS) effectively navigates the vast solution space, thereby significantly improving the efficiency of retrosynthetic planning [40, 18]. Alternatively, Retro* [6] models the search problem as an AND-OR tree where AND nodes and OR nodes alternate, employing an A*-like heuristic to guide the search.

Among existing works, earlier studies adopted a context-free expansion policy (i.e., the single-step model) in which the context information of partially explored synthesis trees is ignored by the predictor [40, 6, 23, 56, 18]. More recently, studies argue that in-context reactions, namely the earlier predicted retrosynthetic steps, can be particularly beneficial to the expansion policy, regardless of the planner's framework. Algorithms like RetroGraph and GNN-Retro [51, 17] utilize graph neural networks to aggregate information from the synthetic route, enabling context-aware cost estimation within the search heuristic. Building on this, FusionRetro [27] explicitly models reactions along synthetic routes as reaction graphs, fusing context embeddings into the single-step predictor to improve planning performance. Furthermore, RetroInText [21] leverages multimodal LLMs for in-context representation learning, utilizing textual descriptions to guide intermediate identification.

In contrast to these representation-focused approaches, our work investigates the potential of fine-tuning LLMs as standalone generative planners via explicit Chain-of-Thought (CoT) reasoning. To the best of our knowledge, LLMs alone have not been deployed as successful multi-step retrosynthetic planners thus far. However, we argue that BioMedGPT-Mol, empowered by its deep molecular expertise and inherent context-learning capabilities, is capable of being fine-tuned as a standalone retrosynthetic planner, bypassing the need for any specialized search algorithms.

In this section, we validate the model's potential by fine-tuning BioMedGPT-Mol on RetroBench dataset[27] to function as an end-to-end planner.

7.1 A Three-stage SFT Strategy for Retrosynthetic Planning

Building upon BioMedGPT-Mol, we employ a three-stage SFT strategy to adapt the model for the retrosynthetic planning task.

In the first stage, we fine-tune the model on the standard training set without CoT [47] to familiarize it with multi-step planning. For data augmentation, we extend the RSMILES technique [58] to multi-step synthesis by aligning SMILES across all reactions and performing a 20-fold augmentation. Specifically, we randomly select a root atom in the target molecule and align the entire synthesis tree relative to that atom.

To enable explicit reasoning for multi-step planning, the second stage introduces a CoT training set. We distill DeepSeek-V3.1 [26] using the complete retrosynthetic tree and all starting materials in SMILES format, prompting it to produce high-level retrosynthetic analyses. These analyses emphasize structural examination, identification of key reaction sites, and potential challenges across the synthesis plan, such as reaction ordering or the need for protecting groups.

Because natural-language reasoning is inherently more ambiguous than SMILES-based answer generation, it induces substantially higher uncertainty. Empirically, we observe that by the end of the second stage, the model's per-token loss on the reasoning component is an order of magnitude higher than its loss on the answer component. This imbalance suggests that optimization is disproportionately influenced by the reasoning signal, potentially overshadowing supervision for the final prediction. Consequently, in the third stage, we rebalance the training objective to refocus the model on accurate reactant prediction. Specifically, within each training sample, we compute the average per-token cross-entropy loss for the reasoning and answer segments independently, denoted as $\mathcal{L}_{\text{thought}}$ and $\mathcal{L}_{\text{answer}}$, respectively. To ensure the model prioritizes the accuracy of the final retrosynthetic plan while maintaining logical coherence, we enforce a weighted objective function defined as:

$$\mathcal{L} = \alpha \cdot \mathcal{L}_{\text{thought}} + (1 - \alpha) \cdot \mathcal{L}_{\text{answer}} \tag{1}$$

where $\alpha = 0.1$ in our implementation. This weighting strategy effectively mitigates the impact of the higher entropy observed in the reasoning tokens, thereby stabilizing the optimization process.

7.2 Performance on RetroBench

To investigate the performance of LLM in retrosynthetic planning task, we evaluate the fine-tuned model on RetroBench [27] and compare it with other representative approaches, including template-based methods [44, 39, 7], semi-template-based methods [42, 43], and template-based methods [22, 37, 27, 21].

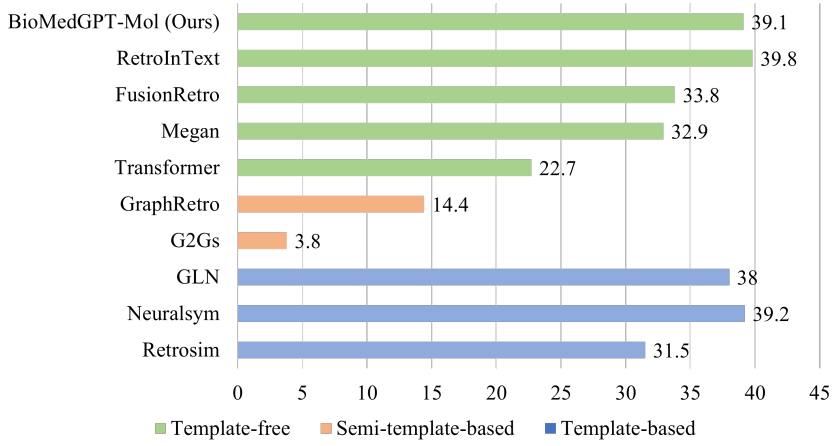

Figure 4: Summary of retrosynthetic planning results for exact match accuracy (%) on RetroBench.

A two-dimensional test-time scaling strategy is adopted, involving reasoning sampling and weighted beam search. We first employ repeated sampling with a non-zero temperature to generate k_s diverse CoT trajectories. For each trajectory, we subsequently perform a partial beam search with a width of k_b to decode the most probable reactant SMILES. The final predictions are ranked by aggregating the local beam scores across all sampled paths using the reciprocal rank sum:

$$Score(y) = \sum_{j \in \mathcal{J}_y} \frac{1}{r_j} \tag{2}$$

where $\mathcal{J}_y$ represents the set of occurrences for reactant y, and r_j denotes its rank within the j-th beam. Figure 4 presents the exact-match accuracy (%) across different methods, illustrating that our approach is highly competitive as a fully end-to-end retrosynthetic planner. Unlike NeuralSym [39], our method is template-free. RetroInText [21] achieves an accuracy of 39.8% by leveraging GPT-4, whereas our 8B-parameter model attains a comparable accuracy of 39.1%. We speculate that scaling the model size will yield substantial performance gains, which we leave for future investigation.

8 Conclusion

In this work, we introduce BioMedGPT-Mol, a molecular language model designed for molecular understanding and generation. To create a molecule-centric research assistant and harness the power of open-source reasoning models with rapid iterative upgrades, we design and implement a multi-task learning strategy for model fine-tuning. Our experimental results demonstrate its remarkable performance, showing that a general-purpose reasoning model can be effectively and efficiently post-trained into a specialized molecular language model through a well-structured multi-task curriculum. On the basis of that, we further explore the challenging retrosynthetic planning task. The proposed three-stage SFT strategy enables it to function as an end-to-end retrosynthetic planner.

BioMedGPT-Mol, with its capabilities in molecular understanding and generation, can assist the entire molecular discovery journey, especially for small molecule drug discovery (Figure 5). Experts can quickly get an overview of the input molecule through molecule captioning and explore further using external databases with the converted molecular names. When they focus on a specific molecule, the 'prediction-optimization-editing' molecular generation cycle can help them more easily obtain a satisfactory molecule. Finally, BioMedGPT-Mol can propose a method for producing the output molecule. We anticipate that molecular language models, such as BioMedGPT-Mol, can significantly enhance expert-in-the-loop molecular research and development.

Furthermore, BioMedGPT-Mol can serve as a foundation for further molecule-centric model research, including optical chemical structure understanding, biomedical multimodal understanding and reasoning, and in-domain biomedical tool planning. Agent systems built with these models can facilitate molecule-centric scientific discovery in an autopilot manner.

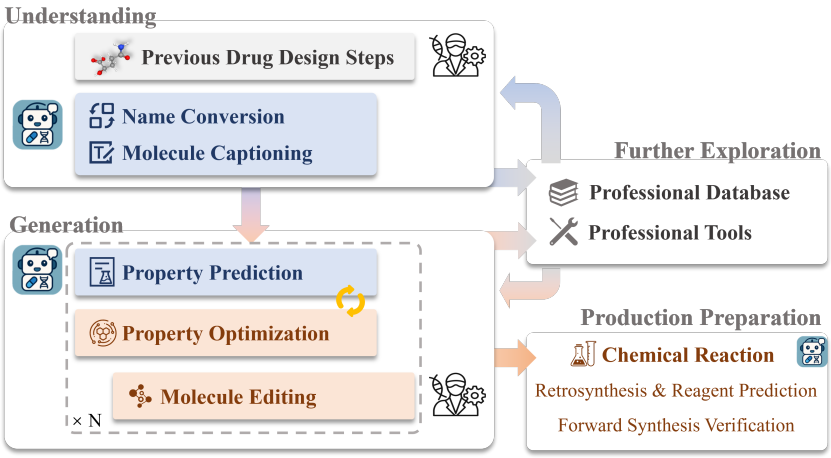

Figure 5: Potential workflow with BioMedGPT-Mol. BioMedGPT-Mol, with its capabilities in molecular understanding and generation, can support the entire molecular discovery journey, particularly in small molecule drug discovery. It can help experts more easily understand new molecules, optimize and generate satisfactory molecules, and propose methods for producing the generated molecules.

References

[1] Josh Achiam, Steven Adler, Sandhini Agarwal, Lama Ahmad, Ilge Akkaya, Florencia Leoni Aleman, Diogo Almeida, Janko Altenschmidt, Sam Altman, Shyamal Anadkat, et al. GPT-4 technical report. *arXiv preprint arXiv:2303.08774*, 2023.

[2] Mistral AI. Mistral 7b. *Mistral AI*, 2023.

[3] Anthropic. The claude 3 model family: Opus, sonnet, haiku. *Anthropic*, 2024.

[4] Anthropic. Claude-3.5. *Anthropic*, 2024.

[5] Akhiad Bercovich, Itay Levy, Izik Golan, Mohammad Dabbah, Ran El-Yaniv, Omri Puny, Ido Galil, Zach Moshe, Tomer Ronen, Najeeb Nabwani, et al. Llama-nemotron: Efficient reasoning models. *arXiv preprint arXiv:2505.00949*, 2025.

[6] Binghong Chen, Chengtao Li, Hanjun Dai, and Le Song. Retro*: learning retrosynthetic planning with neural guided a* search. In *Proceedings of the 37th International Conference on Machine Learning*. JMLR.org, 2020.

[7] Hanjun Dai, Chengtao Li, Connor Coley, Bo Dai, and Le Song. Retrosynthesis prediction with conditional graph logic network. In *Advances in Neural Information Processing Systems*, pages 8870–8880, 2019.

[8] Google Deepmind. Gemini-1.5-pro. *Google Deepmind*, 2024.

[9] Vishal Dey, Xiao Hu, and Xia Ning. $gellm^{3o}$: Generalizing large language models for multi-property molecule optimization. *arXiv preprint arXiv:2502.13398*, 2025.

[10] Carl Edwards, Tuan Lai, Kevin Ros, Garrett Honke, Kyunghyun Cho, and Heng Ji. Translation between molecules and natural language. *arXiv preprint arXiv:2204.11817*, 2022.

[11] Carl Edwards, Qingyun Wang, Lawrence Zhao, and Heng Ji. L+M-24: Building a dataset for language+ molecules@ acl 2024. *arXiv preprint arXiv:2403.00791*, 2024.

[12] Siqi Fan, Yuguang Xie, Bowen Cai, Ailin Xie, Gaochao Liu, Mu Qiao, Jie Xing, and Zaiqing Nie. OCSU: Optical chemical structure understanding for molecule-centric scientific discovery. *arXiv preprint arXiv:2501.15415*, 2025.

[13] Yin Fang, Xiaozhuan Liang, Ningyu Zhang, Kangwei Liu, Rui Huang, Zhuo Chen, Xiaohui Fan, and Huajun Chen. Mol-instructions: A large-scale biomolecular instruction dataset for large language models. *arXiv preprint arXiv:2306.08018*, 2023.

[14] Kaitlyn M Gayvert, Neel S Madhukar, and Olivier Elemento. A data-driven approach to predicting successes and failures of clinical trials. *Cell chemical biology*, 23(10):1294–1301, 2016.

[15] Daya Guo, Dejian Yang, Haowei Zhang, Junxiao Song, Ruoyu Zhang, Runxin Xu, Qihao Zhu, Shirong Ma, Peiyi Wang, Xiao Bi, et al. Deepseek-r1: Incentivizing reasoning capability in llms via reinforcement learning. *arXiv preprint arXiv:2501.12948*, 2025.

[16] Taicheng Guo, Bozhao Nan, Zhenwen Liang, Zhichun Guo, Nitesh Chawla, Olaf Wiest, Xiangliang Zhang, et al. What can large language models do in chemistry? a comprehensive benchmark on eight tasks. *Advances in Neural Information Processing Systems*, 36:59662–59688, 2023.

[17] Peng Han, Peilin Zhao, Chan Lu, Junzhou Huang, Jiaxiang Wu, Shuo Shang, Bin Yao, and Xiangliang Zhang. Gnn-retro: Retrosynthetic planning with graph neural networks. *Proceedings of the AAAI Conference on Artificial Intelligence*, 36(4):4014–4021, 2022.

[18] Siqi Hong, Hankz Hankui Zhuo, Kebing Jin, Guang Shao, and Zhanwen Zhou. Retrosynthetic planning with experience-guided Monte Carlo tree search. *Communications Chemistry*, 6(1):120, 2023.

[19] Kevin Maik Jablonka, Philippe Schwaller, Andres Ortega-Guerrero, and Berend Smit. Leveraging large language models for predictive chemistry. *Nature Machine Intelligence*, 6(2):161–169, 2024.

[20] Aaron Jaech, Adam Kalai, Adam Lerer, Adam Richardson, Ahmed El-Kishky, Aiden Low, Alec Helyar, Aleksander Madry, Alex Beutel, Alex Carney, et al. Openai o1 system card. *arXiv preprint arXiv:2412.16720*, 2024.

[21] Chenglong Kang, Xiaoyi Liu, and Fei Guo. Retrointext: A multimodal large language model enhanced framework for retrosynthetic planning via in-context representation learning. In *The Thirteenth International Conference on Learning Representations*, 2025.

[22] Pavel Karpov, Guillaume Godin, and Igor V. Tetko. A transformer model for retrosynthesis. In *Artificial Neural Networks and Machine Learning – ICANN 2019: Workshop and Special Sessions: 28th International Conference on Artificial Neural Networks, Munich, Germany, September 17–19, 2019, Proceedings*, page 817–830, Berlin, Heidelberg, 2019. Springer-Verlag.

[23] Akihiro Kishimoto, Beat Buesser, Bei Chen, and Adi Botea. *Depth-first proof-number search with heuristic edge cost and application to chemical synthesis planning*. Curran Associates Inc., Red Hook, NY, USA, 2019.

[24] Hao Li, He Cao, Bin Feng, Yanjun Shao, Xiangru Tang, Zhiyuan Yan, Li Yuan, Yonghong Tian, and Yu Li. Beyond chemical qa: Evaluating llm's chemical reasoning with modular chemical operations. *arXiv preprint arXiv:2505.21318*, 2025.

[25] Jiatong Li, Junxian Li, Yunqing Liu, Dongzhan Zhou, and Qing Li. TOMG-Bench: Evaluating llms on text-based open molecule generation. *arXiv preprint arXiv:2412.14642*, 2024.

[26] Aixin Liu, Bei Feng, Bing Xue, Bingxuan Wang, Bochao Wu, Chengda Lu, Chenggang Zhao, Chengqi Deng, Chenyu Zhang, Chong Ruan, et al. Deepseek-v3 technical report. *arXiv preprint arXiv:2412.19437*, 2024.

[27] Songtao Liu, Zhengkai Tu, Minkai Xu, Zuobai Zhang, Lu Lin, Rex Ying, Jian Tang, Peilin Zhao, and Dinghao Wu. Fusionretro: Molecule representation fusion via in-context learning for retrosynthetic planning. In *International Conference on Machine Learning*, 2023.

[28] Michael Luo, Sijun Tan, Justin Wong, Xiaoxiang Shi, William Y Tang, Manan Roongta, Colin Cai, Jeffrey Luo, Tianjun Zhang, Li Erran Li, et al. Deepscaler: Surpassing o1-preview with a 1.5 b model by scaling rl. *Notion Blog*, 2025.

[29] Yizhen Luo, Jiahuan Zhang, Siqi Fan, Kai Yang, Yushuai Wu, Mu Qiao, and Zaiqing Nie. BioMedGPT: Open multimodal generative pre-trained transformer for biomedicine. *arXiv preprint arXiv:2308.09442*, 2023.

[30] Ines Filipa Martins, Ana L Teixeira, Luis Pinheiro, and Andre O Falcao. A bayesian approach to in silico blood-brain barrier penetration modeling. *Journal of chemical information and modeling*, 52(6): 1686–1697, 2012.

[31] Adrian Mirza, Nawaf Alampara, Martiño Ríos-García, Mohamed Abdelalim, Jack Butler, Bethany Connolly, Tunca Dogan, Marianna Nezhurina, Bünyamin Şen, Santosh Tirunagari, et al. ChemPile: A 250gb diverse and curated dataset for chemical foundation models. *arXiv preprint arXiv:2505.12534*, 2025.

[32] David L Mobley and J Peter Guthrie. Freesolv: a database of experimental and calculated hydration free energies, with input files. *Journal of computer-aided molecular design*, 28(7):711–720, 2014.

[33] Siddharth M Narayanan, James D Braza, Ryan-Rhys Griffiths, Albert Bou, Geemi Wellawatte, Mayk Caldas Ramos, Ludovico Mitchener, Samuel G Rodriques, and Andrew D White. Training a scientific reasoning model for chemistry. *arXiv preprint arXiv:2506.17238*, 2025.

[34] Qizhi Pei, Wei Zhang, Jinhua Zhu, Kehan Wu, Kaiyuan Gao, Lijun Wu, Yingce Xia, and Rui Yan. BioT5: Enriching cross-modal integration in biology with chemical knowledge and natural language associations. *arXiv preprint arXiv:2310.07276*, 2023.

[35] Salwa K Poole and Colin F Poole. Separation methods for estimating octanol–water partition coefficients. *Journal of Chromatography B*, 797(1-2):3–19, 2003.

[36] Kohulan Rajan, Achim Zielesny, and Christoph Steinbeck. STOUT: Smiles to iupac names using neural machine translation. *Journal of Cheminformatics*, 13(1):34, 2021.

[37] Mikołaj Sacha, Mikołaj Błaż, Piotr Byrski, Paweł Dąbrowski-Tumański, Mikołaj Chromiński, Rafał Loska, Paweł Włodarczyk-Pruszyński, and Stanisław Jastrzębski. Molecule edit graph attention network: Modeling chemical reactions as sequences of graph edits. *Journal of Chemical Information and Modeling*, 61(7):3273–3284, 2021. PMID: 34251814.

[38] Philippe Schwaller, Teodoro Laino, Théophile Gaudin, Peter Bolgar, Christopher A Hunter, Costas Bekas, and Alpha A Lee. Molecular transformer: a model for uncertainty-calibrated chemical reaction prediction. *ACS central science*, 5(9):1572–1583, 2019.

[39] Marwin HS Segler and Mark P Waller. Neural-symbolic machine learning for retrosynthesis and reaction prediction. *Chemistry–A European Journal*, 23(25):5966–5971, 2017.

[40] Marwin H. S. Segler, Mike Preuss, and Mark P. Waller. Planning chemical syntheses with deep neural networks and symbolic AI. *Nature*, 555(7698):604–610, 2018.

[41] Yu Shee, Anton Morgunov, Haote Li, and Victor S. Batista. Directmultistep: Direct route generation for multistep retrosynthesis. *Journal of Chemical Information and Modeling*, 65(8):3903–3914, 2025.

[42] Chence Shi, Minkai Xu, Hongyu Guo, Ming Zhang, and Jian Tang. A graph to graphs framework for retrosynthesis prediction. In *International Conference on Machine Learning*, 2020.

[43] Vignesh Ram Somnath, Charlotte Bunne, Connor W. Coley, Andreas Krause, and Regina Barzilay. Learning graph models for retrosynthesis prediction. In *Thirty-Fifth Conference on Neural Information Processing Systems*, 2021.

[44] Yijia Sun and Nikolaos V Sahinidis. Computer-aided retrosynthetic design: fundamentals, tools, and outlook. *Current Opinion in Chemical Engineering*, 35:100721, 2022.

[45] Ross Taylor, Marcin Kardas, Guillem Cucurull, Thomas Scialom, Anthony Hartshorn, Elvis Saravia, Andrew Poulton, Viktor Kerkez, and Robert Stojnic. Galactica: A large language model for science. *arXiv preprint arXiv:2211.09085*, 2022.

[46] Kimi Team, Angang Du, Bofei Gao, Bowei Xing, Changjiu Jiang, Cheng Chen, Cheng Li, Chenjun Xiao, Chenzhuang Du, Chonghua Liao, et al. Kimi k1. 5: Scaling reinforcement learning with llms. *arXiv preprint arXiv:2501.12599*, 2025.

[47] Jason Wei, Xuezhi Wang, Dale Schuurmans, Maarten Bosma, brian ichter, Fei Xia, Ed Chi, Quoc V Le, and Denny Zhou. Chain-of-thought prompting elicits reasoning in large language models. In *Advances in Neural Information Processing Systems*, pages 24824–24837. Curran Associates, Inc., 2022.

[48] David Weininger. SMILES, a chemical language and information system. 1. introduction to methodology and encoding rules. *Journal of chemical information and computer sciences*, 28(1):31–36, 1988.

[49] Andrew D White, Glen M Hocky, Heta A Gandhi, Mehrad Ansari, Sam Cox, Geemi P Wellawatte, Subarna Sasmal, Ziyue Yang, Kangxin Liu, Yuvraj Singh, et al. Assessment of chemistry knowledge in large language models that generate code. *Digital Discovery*, 2(2):368–376, 2023.

[50] Zhenqin Wu, Bharath Ramsundar, Evan N Feinberg, Joseph Gomes, Caleb Geniesse, Aneesh S Pappu, Karl Leswing, and Vijay Pande. MoleculeNet: a benchmark for molecular machine learning. *Chemical science*, 9(2):513–530, 2018.

[51] Shufang Xie, Rui Yan, Peng Han, Yingce Xia, Lijun Wu, Chenjuan Guo, Bin Yang, and Tao Qin. Retrograph: Retrosynthetic planning with graph search. In *Proceedings of the 28th ACM SIGKDD Conference on Knowledge Discovery and Data Mining*, page 2120–2129. ACM, 2022.

[52] An Yang, Anfeng Li, Baosong Yang, Beichen Zhang, Binyuan Hui, Bo Zheng, Bowen Yu, Chang Gao, Chengen Huang, Chenxu Lv, et al. Qwen3 technical report. *arXiv preprint arXiv:2505.09388*, 2025.

[53] Geyan Ye, Xibao Cai, Houtim Lai, Xing Wang, Junhong Huang, Longyue Wang, Wei Liu, and Xiangxiang Zeng. DrugAssist: A large language model for molecule optimization. *Briefings in Bioinformatics*, 26(1): bbae693, 2025.

[54] Botao Yu, Frazier N Baker, Ziqi Chen, Xia Ning, and Huan Sun. LlaSMol: Advancing large language models for chemistry with a large-scale, comprehensive, high-quality instruction tuning dataset. *arXiv preprint arXiv:2402.09391*, 2024.

[55] Kevin Yu, Jihye Roh, Ziang Li, Wenhao Gao, Runzhong Wang, and Connor W. Coley. Double-ended synthesis planning with goal-constrained bidirectional search. In *Advances in Neural Information Processing Systems*, pages 112919–112949. Curran Associates, Inc., 2024.

[56] Yemin Yu, Ying Wei, Kun Kuang, Zhengxing Huang, Huaxiu Yao, and Fei Wu. Grasp: Navigating retrosynthetic planning with goal-driven policy. In *Advances in Neural Information Processing Systems*, pages 10257–10268. Curran Associates, Inc., 2022.

[57] Di Zhang, Wei Liu, Qian Tan, Jingdan Chen, Hang Yan, Yuliang Yan, Jiatong Li, Weiran Huang, Xiangyu Yue, Wanli Ouyang, et al. ChemLLM: A chemical large language model. *arXiv preprint arXiv:2402.06852*, 2024.

[58] Zipeng Zhong, Jie Song, Zunlei Feng, Tiantao Liu, Lingxiang Jia, Shaolun Yao, Min Wu, Tingjun Hou, and Mingli Song. Root-aligned smiles: a tight representation for chemical reaction prediction. *Chemical Science*, 13(31):9023–9034, 2022.

[59] Gengmo Zhou, Zhifeng Gao, Qiankun Ding, Hang Zheng, Hongteng Xu, Zhewei Wei, Linfeng Zhang, and Guolin Ke. Uni-Mol: A universal 3d molecular representation learning framework. *ICLR*, 2023.